Chandra probes the X-ray variability of M51 ULX-7: evidence of propeller transition and X-ray dips on orbital periods

Georgios Vasilopoulos,[1] Filippos Koliopanos,[2] Frank Haberl,[3] Helena Treiber,[1,4] Murray Brightman,[5] Hannah P. Earnshaw,[5] and Andrés Gúrpide[2]

[1]*Department of Astronomy, Yale University, PO Box 208101, New Haven, CT 06520-8101, USA*
[2]*Université de Toulouse; UPS-OMP; IRAP, 31058 Toulouse, France*
[3]*Max-Planck-Institut für extraterrestrische Physik,Giessenbachstraße, 85748 Garching, Germany*
[4]*Department of Physics and Astronomy, Amherst College, C025 New Science Center, 25 East Dr., Amherst, MA 01002-5000, USA*
[5]*Cahill Center for Astronomy and Astrophysics, California Institute of Technology, 1216 East California Boulevard, Pasadena,CA 91125, USA*

ABSTRACT

We report on the temporal properties of the ULX pulsar M51 ULX-7 inferred from the analysis of the 2018-2020 *Swift*/XRT monitoring data and archival Chandra data obtained over a period of 33 days in 2012. We find an extended low flux state, which might be indicative of propeller transition, lending further support to the interpretation that the NS is rotating near equilibrium. Alternatively, this off state could be related to a variable super-orbital period. Moreover, we report the discovery of periodic dips in the X-ray light curve that are associated with the binary orbital period. The presence of the dips implies a configuration where the orbital plane of the binary is closer to an edge on orientation, and thus demonstrates that favorable geometries are not necessary in order to observe ULX pulsars. These characteristics are similar to those seen in prototypical X-ray pulsars like Her X-1 and SMC X-1 or other ULX pulsars like NGC 5907 ULX1.

1. INTRODUCTION

Ultra luminous X-ray (ULX) sources (Kaaret et al. 2017) are off-nuclear extra-galactic X-ray binary systems with an apparent isotropic luminosity that exceeds the Eddington limit for an accretion powered, stellar mass black hole (i.e. $L_X > 10^{39}$ erg s^{-1}). Given their high luminosity ULXs were thought to host the elusive intermediate-mass black holes. Remarkably, within the last years there has been undisputed evidence that at least a few of these systems are powered by accreting highly magnetized neutron stars (NS); these are known as ULX pulsars (ULXPs, Bachetti et al. 2014; Fürst et al. 2016; Israel et al. 2017; Israel et al. 2017; Carpano et al. 2018; Rodríguez Castillo et al. 2020). This discovery is consistent with theoretical predictions (e.g. Basko & Sunyaev 1976; Mushtukov et al. 2015) that argue that NSs can break the barrier set by the Eddington limit ($L_{\rm Edd} \sim 1.4 \times 10^{38} M/M_\odot$ erg/s) for strong magnetic fields (B). Moreover, an increasing number of authors have put forward the proposition that a major fraction of ULXs are powered by NSs rather than black holes (e.g. King et al. 2017; Koliopanos et al. 2017; Walton et al. 2018).

For a standard accretion disk (Shakura & Sunyaev 1973), as the accretion rate reaches the Eddington limit, the radiation pressure dominates the inner part of the accretion disk, causing a large fraction of the accreted material to be lost through outflows (Poutanen et al. 2007). Material is expelled inside the spherization radius $R_{\rm sph}$, and the outflow is not spherical but forms a funnel-like structure (see Fig. 1). In the context of ULXPs, the disk is truncated at the magnetospheric radius $R_{\rm M}$. For high B values, truncation can therefore occur outside $R_{\rm sph}$. However, it has been proposed that

Corresponding author: Georgios Vasilopoulos
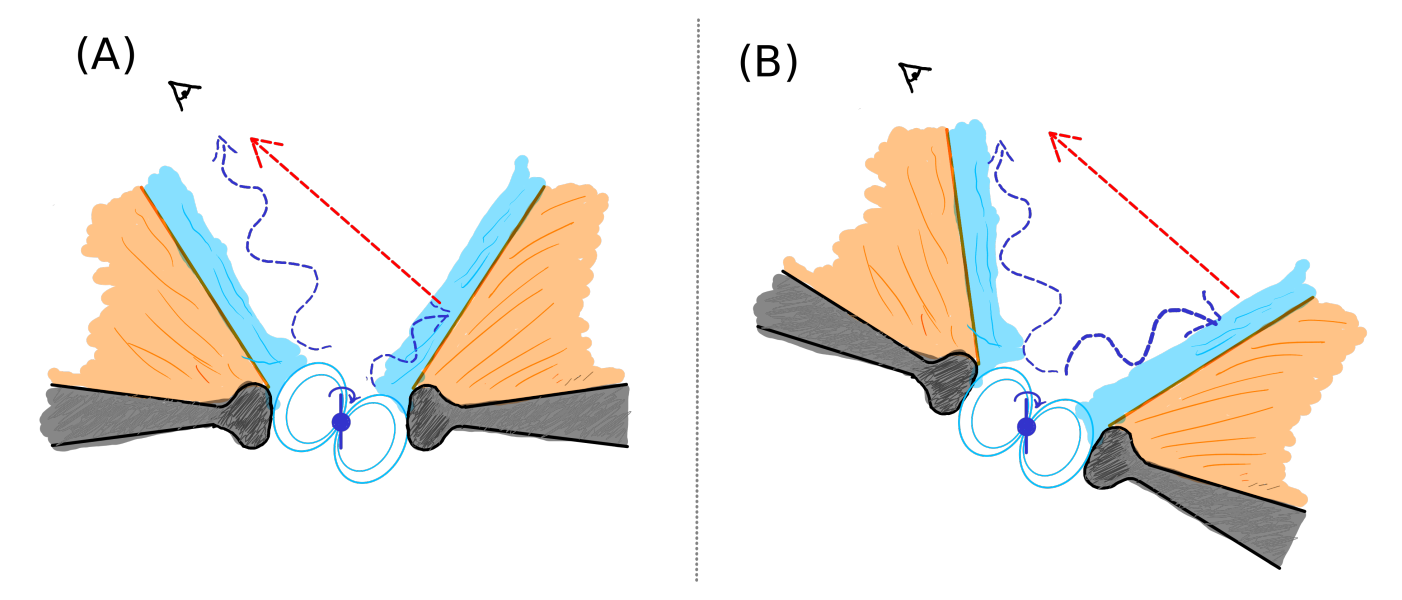georgios.vasilopoulos@yale.edu

Figure 1. Schematic of outflows from an accretion disk during super-Eddington accretion. Outflows can start from the disk (i.e. orange shade), or even inside the magnetosphere (i.e. cyan shade) given the super-Eddington luminosity. The walls of the outflow create a funnel and an observer can see the central source if it is in a favorable orientation (i.e. left panel). The pulsed emission is shown with blue dotted lines, while reprocessed emission is shown with red dotted lines. Given the extent of the funnel, coherent pulsations are diluted, while the spectral shape of the emission should also alter. If the disk precesses, the funnel also follows the same motion, and thus the observer sees a super-orbital modulation. If the observer's line of sight is obscured by the funnel walls, then only non-pulsating emission from the funnel walls should be visible (i.e. right panel).

outflows could form in a similar manner inside $R_{\rm M}$, as material is accreted onto the NS via the magnetic field lines (King et al. 2017).

Super-orbital modulation of ULXs is possible through precession of the funnel (Dauser et al. 2017). For three known ULXPs (M51 ULX-7, M82 X-2 and NGC 5907 ULX1) super-orbital periodicities (40 d, 60 d and 78 d, respectively) are evident in their X-ray light curves (see Brightman et al. 2020, and references therein). The observed flux ($F_{\rm X}$) during a super-orbital cycle can vary by a factor of 100, but there has been no concrete evidence for spectral changes indicating accretor-to-propeller transitions (Illarionov & Sunyaev 1975). These transitions occur when the inner disc radius (i.e. the magnetosphere of the NS) becomes larger than the coro-tation radius of the NS, the centrifugal drag causes material to be propelled away instead of accreted. Alternatively, the changes in $F_{\rm X}$ can be due to obscuration by a precessing accretion disk and a funnel formed by optically thick outflows (Middleton et al. 2018). A firm confirmation of this scenario has been shown in the case of NGC 300 ULX1, where a stable spin-up rate has been maintained during epochs of variable $F_{\rm X}$ (Vasilopoulos et al. 2019). However, the engine behind precession is still unclear; it could be the tidal force from the massive companion star, the interaction with the magnetosphere of the NS, the irradiation of the warped disc, or even the NS free precession (see Vasilopoulos et al. 2020a, and ref-

erences within). Constraints in theoretical models can only be derived by monitoring ULXPs and their super-orbital periodicity, the study of the stability of this periodicity, and the occurrence of on and off states. One of the unanswered fundamental questions about ULXPs is if their X-ray emission is beamed towards the observer, and what is the beaming factor, i.e. apparent luminosity is larger than the true on $L_{\rm app}=bL$. For a narrow funnel (see Fig. 1) beaming could be very strong, while for wide funnels the beaming factor could be smaller than 2. This means that the bolometric X-ray emission of the source is only overestimated by a small factor. Given the lack of physically self-consistent spectral models and the degeneracy of phenomenological ones (e.g. Koliopanos et al. 2017, 2019), we should perhaps look at temporal properties for observational constraints on b.

Gúrpide et al. (2021) have processed archival data of 17 ULXs to investigate their long-term X-ray spectral evolution. Motivated by their work and using the products of their analysis, we studied the variability of M51 ULX-7, the only ULXP with an orbit that can be continuously monitored by X-ray observatories (Townsend & Charles 2020). M51 ULX-7 is a ULXP (Rodríguez Castillo et al. 2020) hosting a NS rotating with a spin period of ∼2.8 s. The binary period is 1.9969 d, while *Swift*/XRT monitoring revealed the presence of a super-orbital modulation with a period of ∼38-39 d (Brightman et al. 2020; Vasilopoulos et al. 2020a). Here
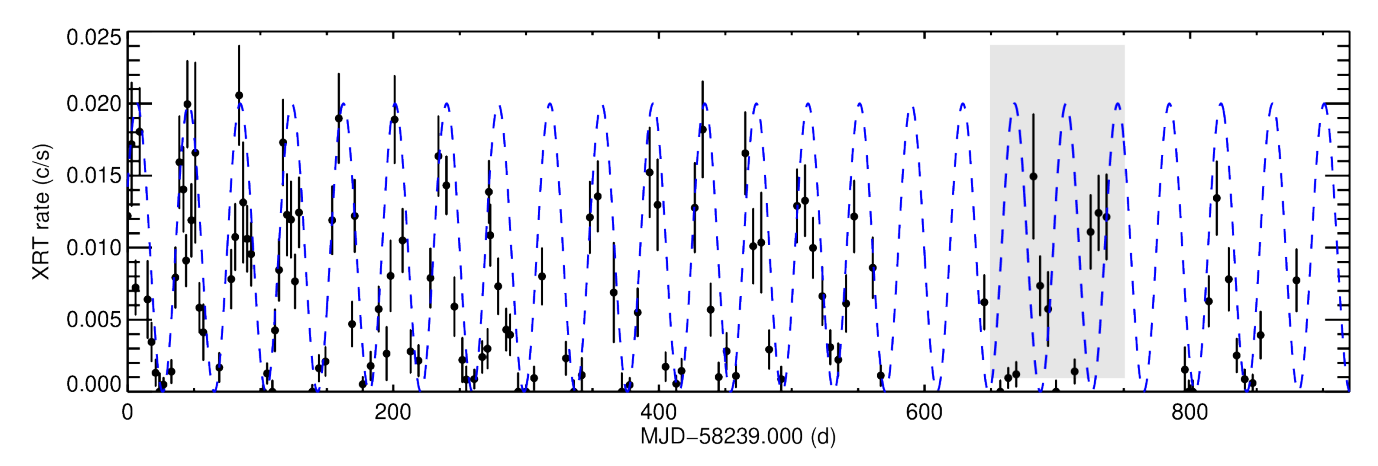
Figure 2. X-ray light curve of M51 ULX-7 based on the 2018-2020 *Swift*/XRT monitoring of the region. Points below 0.005 c/s may be considered as non-detection or upper limits as they correspond to less than ∼5-10 total counts. A sinusoidal curve with a period of 38.86 d is plotted to guide the eye.
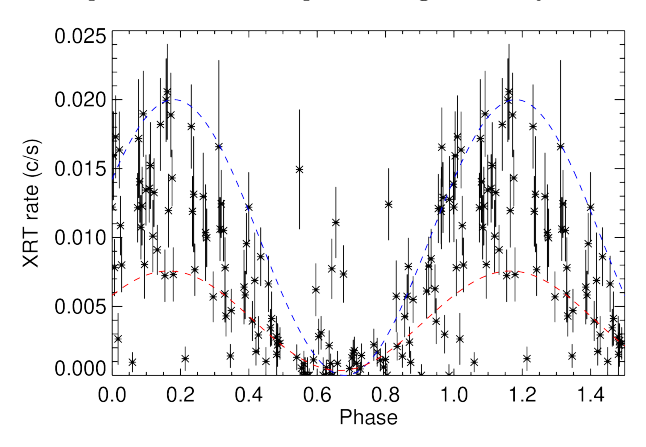

Figure 3. X-ray lightcurve of Fig. 2 folded for the super-orbital period of 38.9 days. Blue dotted curve is same as Fig. 2. Red line is scaled to match the lower flux points through the super-orbital cycle. Most points follow the super-orbital trend, while few outliers are mainly from observations between MJD 58900-59000 d (see shaded area in Fig. 2).

we report on the discovery of an irregular off-state within the super-orbital cycle of M51 ULX-7 and the discovery of periodic dips in the X-ray light curve computed from archival Chandra data. The detection of eclipses offers new insights onto the geometrical configuration of ULXPs, and could provide an independent constraint on the beaming factor of M51 ULX-7.

2. DATA ANALYSIS & RESULTS

2.1. *Probing the super-orbital modulation*

For this study we used X-ray data from the M51 monitoring (Brightman et al. 2020) by the Neil Gehrels *Swift* Observatory (Gehrels et al. 2004) X-ray Telescope (XRT, Burrows et al. 2005). *Swift*/XRT data were analysed following the pipeline developed by Brightman

et al. (2020). To estimate an updated super-orbital period we computed the Lomb-Scargle (LS) periodogram (Scargle 1982) for the 2018-2020 data shown in Fig. 2. A period of ∼38.86 d was found. A systematic uncertainty on the derivation of the super-orbital period has to do with the treatment of marginal detections by *Swift*/XRT. By following Vasilopoulos et al. (2020a) many low flux points are consistent with upper limits. By ignoring all lower flux points with rates smaller than 0.005 c/s, the LS periodogram yields a periodicity of 38.94 d. The difference between the two methods may be considered as an estimate of the uncertainty of the super-orbital period. Thus the super-orbital period should be ∼38.9 d, while the super-orbital maximum flux is expected at MJD 58246.017±N×38.9 d, where N is an integer. Compared to the previous studies of M51 ULX-7 (see, Vasilopoulos et al. 2020a; Brightman et al. 2020), a super-orbital periodicity is evident in the updated data set. However, for a 100 day interval around MJD 58900-59000 d the observed modulation appears to fall out of phase compared to the general trend (see shaded area in Fig. 2), before returning to the normal phase at a later time (i.e. around MJD 59040 d).

M51 was observed by Chandra 16 times. Most of these observations have short exposure times (e.g. ∼20 ks) and thus only contribute to the study of the variability of M51 ULX-7 on timescales of a few hours (i.e. 2 hour long dips reported by Liu et al. 2002). M51 was observed by Chandra between 2012 September 9 and October 10 (PI: Kuntz) with a few long visits (i.e. >100 ks). Earnshaw et al. (2016) analysed the 2012 data and reported on the properties of M51 ULX-7, but the X-ray light curves were not presented in their work. In Table 1 we present the Chandra observations that we used in our analysis, these are C6-C12 as defined

in Table 1 of Earnshaw et al. (2016). Data reduction was performed with the CIAO software (Fruscione et al. 2006). For creation lightcurves, the source (background) events were extracted from circular regions with 3 (20) arcsec radius (following Earnshaw et al. 2016). We used standard FTOOLS scripts to perform event selection and create light curves. For the light curve we used a 6000 s binning to compromise between getting acceptable statistics and sufficient timing resolution (see Fig. 4). To investigate spectral changes we estimated the spectral Hardness Ratio (HR) from each 6000 s interval. We define HR as the ratio of the difference over the sum of the number of counts in two subsequent energy bands: $HR = (R_{i+1} - R_i)/(R_{i+1} + R_i)$, where R_i is the background-subtracted count rate in a specific energy band (i.e. 0.3-1.5 keV and 1.5-8.0 keV). HRs were computed with a Bayesian estimator tool (BEHR; Park et al. 2006).

In Fig. 4 we plot the X-ray light curve obtained from the Chandra observations in September 2012. The modulation looks consistent with the reported 38.9 d super-orbital modulation of M51 ULX-7 (Vasilopoulos et al. 2020a). To test this we extrapolated the super-orbital solution derived by fitting a sinusoidal function to the *Swift*/XRT monitoring data, as shown with a blue line in Fig. 2. We scaled the function by a factor of 3, which is the ratio of the ACIS-S to XRT spectral response given the spectral properties reported by Earnshaw et al. (2016), i.e. an absorbed power-law with $\Gamma = 1.5$ and $N_H = 1.5 \times 10^{21} cm^{-2}$. The result is shown in Fig. 4 by the dashed blue line. For clarity, we also plot a sinusoidal function computed for the upper limit of the super-orbital period, i.e. 38.94 d. The agreement with the Chandra data is good for the first part of the light curve. However, during the final Chandra observation (obsid: 15553) the flux remained at a low level. To further investigate the drop in flux within the last observation we derived accurate count rates for each Chandra pointing. We performed source detection using the CIAO wavdetect tool that implements a wavelet analysis on the X-ray images. The resulted count rates are given in Table 1. The drop in flux seen around MJD 56210 (obsid: 15553) can be compared with observations taken about 15 days earlier (obsid: 13815), when the flux should have been similar according to the super-orbital modulation. Thus we find that on MJD 56210 the flux of M51 ULX-7 is $\sim$80 times lower than expected.

2.2. *Detection of periodic X-ray dips*

The Chandra light curve shows fast variability on timescales of a few 1000 s, which is consistent with other studies of the system (Earnshaw et al. 2016; Liu et al.

Table 1. Chandra Observing log

Obsid[a]	Date	Exposure	Rate[b]
		ks	10^{-2} c/s
13812	2012-09-12	159	5.07±0.06
13813	2012-09-09	181	6.00±0.06
13814	2012-09-22	192	3.88±0.05
13815	2012-09-23	68	2.58±0.06
13816	2012-09-26	74	0.65±0.03
15496	2012-09-19	42	4.44±0.10
15553	2012-10-10	38	0.032±0.010

[a] All data were obtained by ACIS-S camera. [b] Net count rates (0.3–8 keV band) derived from the wavdetect tool.

2002). In particular Liu et al. (2002) claimed the presence of a 2 hour periodicity in early Chandra data, that however only had 20 ks exposure time. Looking at isolated chunks of data it is easy to find such trends, like dips and flares, that nevertheless could be random in nature. However, knowing that the system has a 1.9969 d orbital period we can guide the eye to identify any patterns. By doing so, we identify that the three strongest dips appear to be periodic. These are marked with vertical red lines in Fig. 4. These three dips are not defined by a single point, but have a structure that resembles a trough. Moreover, the first of these appear to be the strongest, but this could also be related to the better statistics obtained in the first Chandra visit, which occurred during the maximum of the super-orbital phase. For visualization purposes, we detrended the lightcurve by fitting a linear regretion model to the data, this is shown in middle panel of Fig. 4. Finally, we have folded the data of the first 15 days with the orbital period (see Fig. 5). The drop in flux during the dips is of the order of 20-30%, but given the intrinsic difficulties in determining a baseline flux, this should be considered as an upper limit.

To investigate the statistical significance of the periodic dips we used various tests based on epoch folding (Davies 1990). The data were folded for a series of test periods, and the resulting profiles were then tested against constancy using a χ^2 test, or a maximization of variance. We used the normalised ratio light curve produced from the three observations where the dips are distinguished (obsids: 13812-4). We folded the ratio light curve for test periods between 0.5 and 3.5 days. Then we binned the folded profile to obtain 20 average measurements (similar to the smoothed profile in Fig. 5) and we calculated the variance of these average values. Finally, we repeated the procedure for 10000 simulated
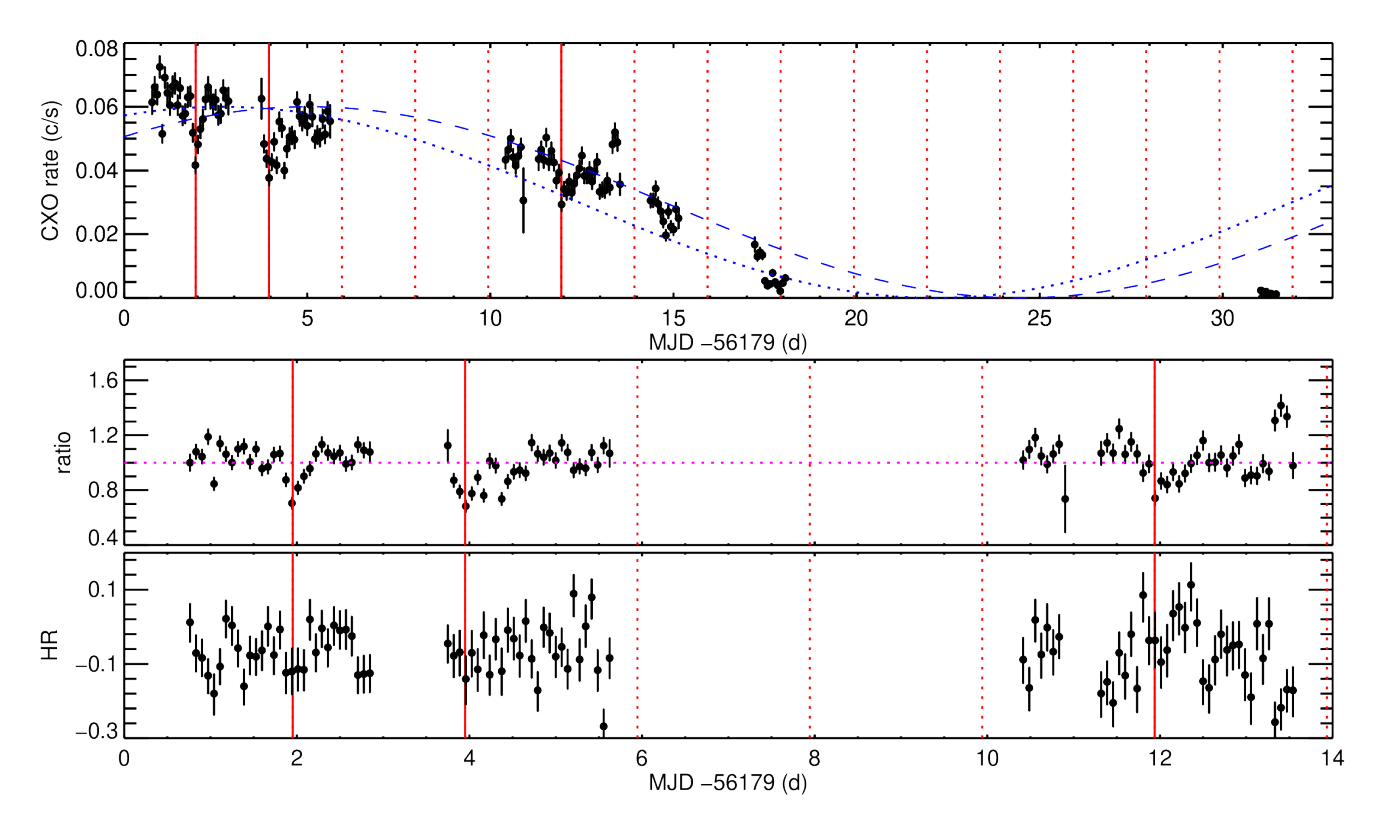
Figure 4. *Upper panel:* X-ray light curve (0.3-8.0 keV) of M51 ULX-7 based on Chandra data obtained in 2012. Events are binned every 6000 s. The vertical dotted lines are phased with the binary orbit of 1.9969 d. There is an indication of periodic flux drops occurring at the same orbital phase. The blue dashed line marks the 38.9 d super-orbital modulation similarly to Fig. 2 and Fig. 3. The dotted line marks the extrapolated solution for a 38.94 d period (see text for details). *Middle panel:* Ratio between Chandra data and a linear model fit to the first 15 days of the Chandra monitoring. *Lower panel:* Spectral hardness evolution estimated by HRs. There is only a marginal indication of spectral softening in the first dip.
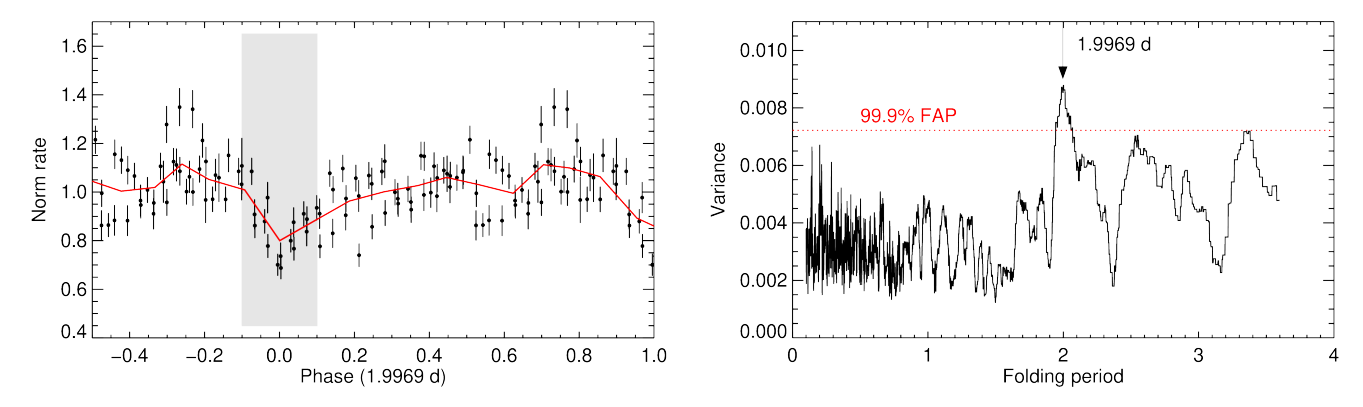

Figure 5. *Left:* Chandra X-ray ratio light curve of M51 ULX-7 folded for the orbital period of the binary. We only used data from obsids 13812-4. Normalised rates were calculated in reference to a linear model fitted to the data. The shaded region marks the approximate duration of the dips. *Right:* Result of epoch-folding method. The maximum variance is found for exactly the orbital period of the system.

data-sets to estimate the false alarm probability. The result is plotted in the right panel of Fig. 5.

Given that the statistical significance of the X-ray dips has been established we should address whether these can be associated with a specific phase of the orbital period. The orbital ephemeris of the system was determined using *XMM-Newton* data obtained between MJD 58251 and 58281 d (Rodríguez Castillo et al. 2020). Given that the Chandra data were obtained about 1100 orbits before that, the ephemeris cannot be extrapolated with enough accuracy to actually compare the predicted transitions of the optical star in front of the NS (i.e. time of ascending nodes: $T_{\rm asc}$) with the X-ray dips. For such comparison we used the the *Swift*/XRT data from the 2018-2020 monitoring of the system (MJD 58000-59125 d). Given that individual observations can span up to one day, we performed source detection to individual snapshots and folded the resulting light curve with the orbital period. We found no evidence of X-ray dips in the *Swift*/XRT orbit-folded light curve. Nevertheless, this should be expected due to the low effective area of XRT and the short exposures that resulted in high uncertainties for individual detections. Specifically for the 170 snapshots where the source was detected, the uncertainties were of the order of 38±15%, i.e. similar or larger than the expected drop in flux during the dips seen in Chandra data (i.e. 15-30%).

3. DISCUSSION

Following the discovery of pulsations originating from the NS in M51 ULX-7, it has been shown that in order to model the spectral and temporal properties of the system self-consistently, the NS should have a very strong magnetic field and should be in the fast rotator regime (Vasilopoulos et al. 2020a). Vasilopoulos et al. (2020a) also argued that the ~39 d super-orbital modulation of the ULXP could be triggered by (or related to) free precession of the NS, which surprisingly requires a NS magnetic field of 3-4×10^{13} G, in quantitative agreement with the spin equilibrium predictions. As a consequence, strong outflows are not expected from the accretion disk (since $R_{\rm M} > R_{\rm sph}$). Thus the opening funnel of any outflow should be large, and as a result we do not expect strong beaming by the system and accretion onto the NS is indeed 10-30 times above the Eddington limit (Vasilopoulos et al. 2020a). In the following paragraphs, we will discuss how the newly reported patterns of X-ray variability can be interpreted and address some of the open questions for M51 ULX-7 and ULXPs, like investigating beaming and the engine behind super-orbital modulation.

3.1. *Propeller transition or an unstable super-orbital clock*

In terms of super-orbital variability, the agreement between the modulation seen in the Chandra data and the phase of the expected maximum of the super-orbital period computed by the *Swift*/XRT monitoring data is remarkable. Especially considering that the *Swift* and Chandra data are separated by about 50 super-orbital cycles. Thus, the drops may be related to a transition to the propeller state, as it is speculated for similar drops in flux seen in NGC 5907 ULX1 (Fürst et al. 2017). This drop in flux is in agreement with the behavior seen by *Swift*/XRT around MJD 55715 d (see Vasilopoulos et al. 2020a), where during a 70 day monitoring M51 ULX-7 was not detected in the final 20 days of the monitoring, when the rise of its flux was expected according to the super-orbital period. However, in both epochs, there are no additional monitoring data to determine the duration of the off state, or investigate if the super-orbital period was different than the one determined by the 2018-2020 monitoring. A similar "off-state" is seen in the *Swift*/XRT data around MJD 58900 d (see Figs. 2, 3), where the flux dropped near zero for 3 consecutive visits. In that case although the super-orbital cycle seemed to be disturbed the super-orbital period returned to its normal beating pace after a few cycles.

A stable super-orbital period would also be in agreement with the requirements of the NS free precession mechanism, as the ratio of super-orbital and NS spin period should be proportional to the NS B field. Since a transition to the propeller regime can occur with minimal change in mass accretion if the accretion disk is truncated near the NS corotation radius, this drop in flux lends further support to the findings of Vasilopoulos et al. (2020a), who proposed that the NS has a magnetic field $\sim 3-7 \times 10^{13}$ G and is rotating near its equilibrium period. Nevertheless, a variable super-orbital period cannot be excluded for M51 ULX-7. If a variable period is confirmed with future monitoring data this would reveal a similar observational behavior to HMXB pulsars like SMC X-1 (Trowbridge et al. 2007).

Assuming that the off-state is associated with propeller transition, we can derive the NS magnetic field B that would be required for the transition to occur. Following Campana et al. (2018) we find that:

$$B = 10^{12} \left(\frac{L_{X,min}}{2 \times 10^{38} erg/s} (P/1s)^{7/3} \xi^{-7/2} \right)^{1/2} G, \quad (1)$$

where ξ is a normalization factor with typical value of 0.5 (however see case of ULXs Chashkina et al. 2019, where ξ can be higher), and $L_{\rm X,min}$ is the minimum luminosity before the propeller transition. Given that the super-

orbital modulation is due to precession (see Fig. 1), its true L_X is similar to the maximum X-ray luminosity within the super-orbital cycle. For M51 ULX-7 this is of the order of 7×10^{39} erg s^{-1} in the 0.3-10.0 keV band (Rodríguez Castillo et al. 2020; Gúrpide et al. 2021), however for ULXPs the bolometric luminosity could be of a factor of 2 higher (Koliopanos et al. 2017; Gúrpide et al. 2021). Moreover, it has already been established that the observed L_X is only boosted by small beaming (Vasilopoulos et al. 2020a), of the order of 2 or less (see also §3.3). Since many of the above uncertainties cancel out, we can adopt a value of $L_{X,min} \sim 7 \times 10^{39}$ erg s^{-1} for propeller transition (but we caution the reader for the above mentioned uncertainties), thus based on equation 1 we find $B \sim 4-9 \times 10^{13}$ G. We note that, depending on the torque model used the propeller transition can occur very close (factor < 2) to the L_X that probes spin equilibrium for a given magnetic field (see comparisons Parfrey et al. 2016; Vasilopoulos et al. 2018). Thus, equation 1 yields a similar magnetic field estimate to the value derived by just assuming the NS is rotating near equilibrium (see discussions for M51 ULX-7 and M82 X-2 Vasilopoulos et al. 2020a; Eksi et al. 2015).

So far we have connected the "off-states" of M51 ULX-7 with the source transitioning from accretor to propeller regime. Thus, during the "off-state" the source has moved way down on the Luminosity gap for X-ray pulsars (i.e., Corbet gap; Corbet 1996). However, given the spin period of ~ 2.8 s such transition should have resulted in a drop[1] in L_X of the order of ~ 330, and not just ~ 80. This discrepancy may be explained if we assume that even at the propeller regime, there is still some residual accretion that can penetrate the magnetophseric barrier (Spruit & Taam 1993), a mechanism that has been supported by theory and simulations (e.g., D'Angelo & Spruit 2012; Parfrey & Tchekhovskoy 2017; Romanova et al. 2018).

An opposing view would be that during the "off-state", M51 ULX-7 is still in the accretor regime. This limit may be used to put a lower limit to the propeller stage assuming that the source is then on the propeller line. By using equation 1 we find $B \sim 5 \times 10^{12}$ G. However, this low B field value posses difficulties in explaining the very low NS spin-up rate ($\dot{P}_{NS}$) observed during maximum X-ray luminosity (Rodríguez Castillo et al. 2020). Given all the observational evidence, to account for this low B value and the observed $\dot{P}_{NS}$, we would need change our basic assumptions (for the accretion disk) in order to

decrease the rate of angular momentum transfer. Inefficient angular momentum transfer may be achieved if the accretion disk is miss-aligned with the NS rotation axis, or the inner disk velocity significantly deviates from the Keplerian approximation.

3.2. *M51 ULX-7 as an ULXP analog of Her X-1*

The study of ULXPs has revealed not only that some host strongly magnetized NSs, but also that this might be the norm for a large fraction of ULXs (Koliopanos et al. 2017; King et al. 2017). Thus, it is natural to look for similarities (and also differences) between individual ULXPs and HMXBs, which host the majority of X-ray pulsars. The NS spin period as well as the orbital and super-orbital periods of M51 ULX-7 (2.8 s, 1.99 d and ~ 40 d), are close to the values (1.24 s, 1.7 d and ~ 35 d) of the prototypical X-ray pulsar Her X-1 (Tananbaum et al. 1972; Katz 1973). In regards to the super-orbital modulation, for both systems it has been proposed that NS free precession could play an important role (Truemper et al. 1986; Staubert et al. 2009; Vasilopoulos et al. 2020a). Another characteristic feature of Her X-1 is the presence of eclipses that coincide with the orbital period of the binary. Our study of M51 ULX-7 found evidence of similar features that occur periodically and could help to further constrain the properties of the system. In order to understand the nature of the X-ray dips in M51 ULX-7 we can thus refer to the plethora of theoretical models proposed for Her X-1. In Her X-1 full eclipses occur when X-rays are obscured by the companion star, however in its X-ray light curve there are characteristic X-ray dips, commonly referred to as *pre-eclipse* or *anomalous dips*. The pre-eclipse dips (2-5 h long) occur before the eclipse and gradually march backward in phase within the super-orbital cycle. Anomalous dips (1-2 h long) occur at the same orbital phase, while there is evidence of cold matter absorption, in contrast to the pre-eclipse dips (Reynolds & Parmar 1995). Theoretical explanations of these dips include dynamical, hydrodynamic and radiative interactions between the accretion stream, the warped accretion disk and the companion star (e.g. Schandl 1996; Shakura et al. 1999). If the stream falls into the warped disk with an angle, the formation of a cold clumpy spray is possible, that in turn will cover the central source once per orbit (Schandl 1996). In this scenario, a turbulent thickening of the warped disk is also possible.

A different cause for the X-ray dips is obscuration by the stellar wind of the companion. For X-ray binaries it is important to take into account the strong X-ray illumination of the companion star that can affect the geometry of the stellar winds. It has been shown that

---

[1] Luminosity jump is propotional to the ratio of the dynamical energy at the NS surface over the corotation radius (Corbet 1996), i.e. $\sim 170 \times (P/1 \text{ s})^{2/3}$

X-ray illumination can cause the formation of a so-called "shadow wind" by the companion in luminous HMXBs (Blondin 1994). By performing 2D hydrodynamic simulations, Blondin (1994) found that for high X-ray luminosities the gas that resides on the stellar surface exposed to the X-ray source will be highly photoionized, and thus halt the formation of a radiative driven wind from that side (see Haberl et al. 1989, for an application to 4U 1700-37). Given that stellar wind can still escape from the other side of the star, enhanced column density is still possible at favorable orientations and orbital phases. In fact, the shadow wind model has been offered as a possible mechanism to explain periodic dips seen during a super-Eddington outburst of SMC X-2 (Li et al. 2016). For systems like Her X-1, the irradiation of the companion star can also depend on the binary orbital phase (Shakura et al. 1999). In this scenario, the (phase dependent) shadowing of the companion by the disk leads to the formation of flows coming out from the orbital plane and could in principle shadow the central source once per orbit.

For M51 ULX-7 it is possible to imagine a similar scenario, where either (or all) of the above mechanisms can provide the necessary conditions to form the X-ray dips under a favorable orientation. Nevertheless, the lack of significant spectral change during the dips (see HRs in Fig. 4), could be an indication of obscuration from a fully ionised material rather than cold matter.

3.3. Constraints on orbit inclination and ULX beaming

At this point, and without further observations of M51 ULX-7 during full orbital cycles, it is not possible to test different models such as those introduced in section 3.2. However, we might test the extreme case where the dips are caused by partial obscuration by material very close to the Roche lobe radius, that perhaps could be at the Lagrangian points or the inner wind of the companion star. The Roche lobe radius, from the vantage point of the NS, will subtend an area on the sky with an angular radius θ, i.e.:

$$\tan(\theta) \approx \frac{R_{\rm RL}}{a} = \frac{0.49q^{2/3}}{0.6q^{2/3} + \ln(1 + q^{1/3})}, \qquad (2)$$

where $R_{\rm RL}$ is the donor radius that has filled its Roche lobe, a is the separation between the donor and the NS, and their ratio depends only on the mass ratio $q = M_{\rm donor}/M_{\rm NS}$ (Eggleton 1983). The mass ratio in M51 ULX-7 is $\gtrsim 6$ (Rodríguez Castillo et al. 2020). Although the mass ratio depends on the orbital inclination i ($i=0$, refers to a face-on system), θ is actually weakly dependent on it. Assuming the companion always fills its Roche lobe, for i 90°-45° we find $\theta \sim 28.2^o - 29.4^o$.

Given that $a \simeq 2R_{\rm RL}$, the duration of an eclipse in a 2 day circular orbit would last $\sim 8\,{\rm h}$ (0.16 in phase), which is comparable to the duration of the dips (see Fig. 5). These estimates show that the companion may indeed obscure a small opening angle from the NS vantage point of view. Nevertheless, it is unclear if this configuration can constrain the opening angle of the funnel walls created by outflow in ULXPs (see Fig. 1). Assuming the funnel axis is fixed perpendicular to the orbital plane, its opening angle should be large enough to allow dips to be created by material in the line of sight. This would mean that the funnel's half opening angle should be $\sim 60^o$ (full opening of $\sim 120^o$). However, given the known super-orbital modulation in M51 ULX-7 and ULXPs in general, the funnel orientation should change within the super-orbital cycle. Thus this would not exclude smaller opening angles for the funnel. Nevertheless, a large opening angle is consistent with the large truncation radius of the disk in M51 ULX-7, that was derived from its temporal properties and is consistent with the NS rotating near equilibrium (e.g. Vasilopoulos et al. 2020a; Erkut et al. 2020). Similar findings that suggest low or no beaming at all have been discussed based on spectro-temporal properties of ULXPs (e.g. NGC 300 ULX-1 Vasilopoulos et al. 2018, 2019), or pulse profile evolution of X-ray pulsars during super-Eddington outbursts (e.g. Koliopanos & Vasilopoulos 2018; Vasilopoulos et al. 2020b). This would mean that the proposed relation between mass accretion rate and beaming factor b, i.e. $b \simeq (\dot{M}/\dot{M}_{\rm edd})^2/73$ (King et al. 2017), would need to be revisited in the context of ULXPs. Small beaming is also consistent with the detection of pulsations in ULXPs, as large beaming factors would otherwise result in very small pulsed fractions (Mushtukov et al. 2020). The above suggest that strong beaming is not needed for ULXPs, and this should be considered in the framework of ULX population synthesis (e.g. Kuranov et al. 2020; Misra et al. 2020; Abdusalam et al. 2020), and perhaps gravitational wave progenitors, that are thought to go through a ULX phase (Marchant et al. 2017).

An important consequence of the discovery of the X-ray dips is that, regardless of assumptions about beaming, it is now evident that ULXPs can be seen even as near edge-on systems. In the literature, ULXs that show X-ray eclipses are often assumed to host BHs (e.g. Urquhart & Soria 2016). Nevertheless, for another confirmed ULXP, NGC 7793 P13, it has been speculated that X-ray dips that appear during its orbital light curve were also evident of an edge-on system (Motch et al. 2014). Thus, future search for pulsations should not be discouraged even for eclipsing ULXs. Finally, another

way of approaching the problem would be to search for optical dips caused by obscuration by the NS and its accretion disk (Maggi et al. 2013). For M51 ULX-7 we can potentially confirm the low inclination via the search for optical eclipses via observations with Hubble or James Webb space telescopes (Gardner et al. 2006).

3.4. *Implications for orbital modulation*

Our findings suggest that the mass accretion rate in M51 ULX-7 is indeed super-Eddington. An implication of high accretion rates in ULXs is the change of the binary orbital period over time (Bachetti et al. 2020). According to Bachetti et al. (2020) the orbital period derivative should be:

$$\dot{P}_{\rm orb} \approx -3.5 \times 10^{-8} \left(\frac{M_{\rm NS}}{1.4 M_\odot} \right)^{-1} \left(\frac{\dot{M}}{100 \dot{M}_{\rm Edd}} \right) \ s/s \quad (3)$$

Given that mass accretion rate for M51 ULX-7 is about $30\dot{M}_{\rm Edd}$, the binary orbit should change by $\sim$0.3 s/y. The binary completes $\sim$180 revolutions per year which would translate to a drift in the epoch of $T_{\rm asc}$ of the order of 30 s/year, or about 250 s between 2012 and 2020. Future observations with X-ray telescopes could help constrain this drift by tracking the eclipses, or pulsar timing techniques (e.g. Bachetti et al. 2020; Rodríguez Castillo et al. 2020).

4. CONCLUSION

By analysing archival Chandra and *Swift*/XRT data we investigated the super-orbital and orbital variability of M51 ULX-7. The 2012 Chandra data obtained within 33 days show an extended low flux state, in contrast to the super-orbital clock the system. A similar low flux state is also seen in the 2020 *Swift*/XRT monitoring data. These off-states might be related to propeller transition similar to ULXP NGC 5907 ULX1. Alternatively they could be indicative of a variable super-orbital period like those in other accreting pulsars (see Her X-1, SMC X-1). Moreover, we have reported the presence of periodic dips in the Chandra X-ray light curve of M51 ULX-7. Although X-ray dips are also seen in bright X-ray binaries (Marelli et al. 2017) and ULXs (Wang et al. 2018), this is the first evidence of such property in ULXPs. The physical origin of the dips remain unclear, however they could be related to a plethora of mechanisms that have been proposed to explain similar features in HMXBs. Our finding demonstrates the need for developing numerical simulations of HMXB systems in the context of super-Eddington accretion and investigating these intriguing phenomena. From an observational point of view, it demonstrates the need for long monitoring observations of ULXPs and ULXs to identify and confirm the presence of features related to orbital modulation. Such combined efforts would help to develop a physically motivated, self-consistent model able to explore the central engines of ULXPs.

REFERENCES

Abdusalam, K., Ablimit, I., Hashim, P., et al. 2020, ApJ, 902, 125, doi: 10.3847/1538-4357/abb5a8

Bachetti, M., Harrison, F. A., Walton, D. J., et al. 2014, Nature, 514, 202, doi: 10.1038/nature13791

Bachetti, M., Maccarone, T. J., Brightman, M., et al. 2020, ApJ, 891, 44, doi: 10.3847/1538-4357/ab6d00

Basko, M. M., & Sunyaev, R. A. 1976, MNRAS, 175, 395

Blondin, J. M. 1994, ApJ, 435, 756, doi: 10.1086/174853

Brightman, M., Earnshaw, H., Fürst, F., et al. 2020, ApJ, 895, 127, doi: 10.3847/1538-4357/ab7e2a

Burrows, D. N., Hill, J. E., Nousek, J. A., et al. 2005, SSRv, 120, 165, doi: 10.1007/s11214-005-5097-2

Campana, S., Stella, L., Mereghetti, S., & de Martino, D. 2018, A&A, 610, A46, doi: 10.1051/0004-6361/201730769

Carpano, S., Haberl, F., Maitra, C., & Vasilopoulos, G. 2018, MNRAS, 476, L45, doi: 10.1093/mnrasl/sly030

Chashkina, A., Lipunova, G., Abolmasov, P., & Poutanen, J. 2019, A&A, 626, A18, doi: 10.1051/0004-6361/201834414

Corbet, R. H. D. 1996, ApJL, 457, L31, doi: 10.1086/309890

D'Angelo, C. R., & Spruit, H. C. 2012, MNRAS, 420, 416, doi: 10.1111/j.1365-2966.2011.20046.x

Dauser, T., Middleton, M., & Wilms, J. 2017, MNRAS, 466, 2236, doi: 10.1093/mnras/stw3304

Davies, S. R. 1990, MNRAS, 244, 93

Earnshaw, H. M., Roberts, T. P., Heil, L. M., et al. 2016, MNRAS, 456, 3840, doi: 10.1093/mnras/stv2945

Eggleton, P. P. 1983, ApJ, 268, 368, doi: 10.1086/160960

Eksi, K. Y., Andac, I. C., Cikintoglu, S., et al. 2015, MNRAS, 448, L40, doi: 10.1093/mnrasl/slu199

Erkut, M. H., Türkoğlu, M. M., Ekşi, K. Y., & Alpar, M. A. 2020, ApJ, 899, 97, doi: 10.3847/1538-4357/aba61b

Fruscione, A., McDowell, J. C., Allen, G. E., et al. 2006, in SPIE Conference Series, ed. D. R. Silva & R. E. Doxsey, Vol. 6270, 62701V, doi: 10.1117/12.671760

Fürst, F., Walton, D. J., Stern, D., et al. 2017, ApJ, 834, 77, doi: 10.3847/1538-4357/834/1/77

Fürst, F., Walton, D. J., Harrison, F. A., et al. 2016, ApJL, 831, L14, doi: 10.3847/2041-8205/831/2/L14

Gardner, J. P., Mather, J. C., Clampin, M., et al. 2006, SSRv, 123, 485, doi: 10.1007/s11214-006-8315-7

Gehrels, N., Chincarini, G., Giommi, P., et al. 2004, ApJ, 611, 1005, doi: 10.1086/422091

Gúrpide, A., Godet, O., Koliopanos, F., Webb, N., & Olive, J.-F. 2021, A&A submitted

Haberl, F., White, N. E., & Kallman, T. R. 1989, ApJ, 343, 409, doi: 10.1086/167714

Illarionov, A. F., & Sunyaev, R. A. 1975, A&A, 39, 185

Israel, G. L., Belfiore, A., Stella, L., et al. 2017, Science, 355, 817, doi: 10.1126/science.aai8635

Israel, G. L., Papitto, A., Esposito, P., et al. 2017, MNRAS, 466, L48, doi: 10.1093/mnrasl/slw218

Kaaret, P., Feng, H., & Roberts, T. P. 2017, ARA&A, 55, 303, doi: 10.1146/annurev-astro-091916-055259

Katz, J. I. 1973, Nature Physical Science, 246, 87, doi: 10.1038/physci246087a0

King, A., Lasota, J.-P., & Kluźniak, W. 2017, MNRAS, 468, L59, doi: 10.1093/mnrasl/slx020

Koliopanos, F., & Vasilopoulos, G. 2018, A&A, 614, A23, doi: 10.1051/0004-6361/201731623

Koliopanos, F., Vasilopoulos, G., Buchner, J., Maitra, C., & Haberl, F. 2019, A&A, 621, A118, doi: 10.1051/0004-6361/201834144

Koliopanos, F., Vasilopoulos, G., Godet, O., et al. 2017, A&A, 608, A47, doi: 10.1051/0004-6361/201730922

Kuranov, A. K., Postnov, K. A., & Yungelson, L. R. 2020, arXiv e-prints, arXiv:2010.03488. https://arxiv.org/abs/2010.03488

Li, K. L., Hu, C. P., Lin, L. C. C., & Kong, A. K. H. 2016, ApJ, 828, 74, doi: 10.3847/0004-637X/828/2/74

Liu, J.-F., Bregman, J. N., Irwin, J., & Seitzer, P. 2002, ApJL, 581, L93, doi: 10.1086/346101

Maggi, P., Haberl, F., Sturm, R., et al. 2013, A&A, 554, A1, doi: 10.1051/0004-6361/201321238

Marchant, P., Langer, N., Podsiadlowski, P., et al. 2017, A&A, 604, A55, doi: 10.1051/0004-6361/201630188

Marelli, M., Tiengo, A., De Luca, A., et al. 2017, ApJL, 851, L27, doi: 10.3847/2041-8213/aa9b2e

Middleton, M. J., Fragile, P. C., Bachetti, M., et al. 2018, MNRAS, 475, 154, doi: 10.1093/mnras/stx2986

Misra, D., Fragos, T., Tauris, T. M., Zapartas, E., & Aguilera-Dena, D. R. 2020, A&A, 642, A174, doi: 10.1051/0004-6361/202038070

Motch, C., Pakull, M. W., Soria, R., Grisé, F., & Pietrzyński, G. 2014, Nature, 514, 198, doi: 10.1038/nature13730

Mushtukov, A. A., Portegies Zwart, S., Tsygankov, S. S., Nagirner, D. I., & Poutanen, J. 2020, arXiv e-prints, arXiv:2011.09710. https://arxiv.org/abs/2011.09710

Mushtukov, A. A., Suleimanov, V. F., Tsygankov, S. S., & Poutanen, J. 2015, MNRAS, 447, 1847, doi: 10.1093/mnras/stu2484

Parfrey, K., Spitkovsky, A., & Beloborodov, A. M. 2016, ApJ, 822, 33, doi: 10.3847/0004-637X/822/1/33

Parfrey, K., & Tchekhovskoy, A. 2017, ApJL, 851, L34, doi: 10.3847/2041-8213/aa9c85

Park, T., Kashyap, V. L., Siemiginowska, A., et al. 2006, ApJ, 652, 610, doi: 10.1086/507406

Poutanen, J., Lipunova, G., Fabrika, S., Butkevich, A. G., & Abolmasov, P. 2007, MNRAS, 377, 1187, doi: 10.1111/j.1365-2966.2007.11668.x

Reynolds, A. P., & Parmar, A. N. 1995, A&A, 297, 747

Rodríguez Castillo, G. A., Israel, G. L., Belfiore, A., et al. 2020, ApJ, 895, 60, doi: 10.3847/1538-4357/ab8a44

Romanova, M. M., Blinova, A. A., Ustyugova, G. V., Koldoba, A. V., & Lovelace, R. V. E. 2018, NewA, 62, 94, doi: 10.1016/j.newast.2018.01.011

Scargle, J. D. 1982, ApJ, 263, 835, doi: 10.1086/160554

Schandl, S. 1996, A&A, 307, 95

Shakura, N. I., Prokhorov, M. E., Postnov, K. A., & Ketsaris, N. A. 1999, A&A, 348, 917. https://arxiv.org/abs/astro-ph/9902146

Shakura, N. I., & Sunyaev, R. A. 1973, A&A, 24, 337

Spruit, H. C., & Taam, R. E. 1993, ApJ, 402, 593, doi: 10.1086/172162

Staubert, R., Klochkov, D., Postnov, K., et al. 2009, A&A, 494, 1025, doi: 10.1051/0004-6361:200810743

Tananbaum, H., Gursky, H., Kellogg, E. M., et al. 1972, ApJL, 174, L143, doi: 10.1086/180968

Townsend, L. J., & Charles, P. A. 2020, MNRAS, 495, 139, doi: 10.1093/mnrasl/slaa078

Trowbridge, S., Nowak, M. A., & Wilms, J. 2007, ApJ, 670, 624, doi: 10.1086/522075

Truemper, J., Kahabka, P., Oegelman, H., Pietsch, W., & Voges, W. 1986, ApJL, 300, L63, doi: 10.1086/184604

Urquhart, R., & Soria, R. 2016, ApJ, 831, 56, doi: 10.3847/0004-637X/831/1/56

Vasilopoulos, G., Haberl, F., Carpano, S., & Maitra, C. 2018, A&A, 620, L12, doi: 10.1051/0004-6361/201833442

Vasilopoulos, G., Lander, S. K., Koliopanos, F., & Bailyn, C. D. 2020a, MNRAS, 491, 4949, doi: 10.1093/mnras/stz3298

Vasilopoulos, G., Petropoulou, M., Koliopanos, F., et al. 2019, MNRAS, 488, 5225, doi: 10.1093/mnras/stz2045

Vasilopoulos, G., Ray, P. S., Gendreau, K. C., et al. 2020b, MNRAS, 494, 5350, doi: 10.1093/mnras/staa991

Walton, D. J., Fürst, F., Heida, M., et al. 2018, ApJ, 856, 128, doi: 10.3847/1538-4357/aab610

Wang, S., Soria, R., Urquhart, R., & Liu, J. 2018, MNRAS, 477, 3623, doi: 10.1093/mnras/sty872